AKADÉMIAI KIADÓ

Acta Microbiologica et Immunologica Hungarica

69 (2022) 2, 109–117

DOI:
10.1556/030.2022.01689

RESEARCH ARTICLE

Linezolid decreases *Staphylococcus aureus* biofilm formation by affecting the IcaA and IcaB proteins

HONGXIA BI, RONG DENG and YANBIN LIU*

Center of Infectious Disease, West China Hospital, Sichuan University, Chengdu, China

Received: December 15, 2021 • Accepted: April 21, 2022
Published online: May 17, 2022

ABSTRACT

Background: The *ica* gene of *Staphylococcus aureus (S. aureus)* plays a vital role in its growth and biofilm formation. Among them, IcaA and IcaB are critical proteins for synthesizing extracellular polysaccharides and biofilms in *S. aureus*. To investigate whether the formation of *S. aureus* biofilms can be inhibited through the IcaA and IcaB proteins by the presence of linezolid. *Methods:* The *icaA* and *icaB* genes of *S. aureus* ATCC 25923 were silenced by homologous recombination. The critical roles of *icaA* and *icaB* in *S. aureus* were analysed by observing the growth curve and biofilm formation after linezolid treatment. Then, the effect of linezolid on the morphology of *S. aureus* was observed by scanning electron microscopy. Finally, the potential binding ability of linezolid to Ica proteins was predicted by molecular docking. *Results:* The *icaA*- and *icaB*-silenced strains were successfully constructed, and the sensitivity of *S. aureus* to linezolid was decreased after *icaA* and *icaB* silencing. Scanning electron microscopy showed that linezolid caused invagination of the *S. aureus* surface and reduced the production of biofilms. Molecular docking results showed that linezolid could bind to IcaA and IcaB proteins. *Conclusion:* IcaA and IcaB are potential targets of linezolid in inhibiting the biofilm formation of *S. aureus* (ATCC 25923).

KEYWORDS

Staphylococcus aureus, biofilm, *icaA, icaB*, linezolid

INTRODUCTION

Bacterial resistance is a serious global problem. In Europe, an estimated 33,000 deaths are attributed to antibiotic-resistant infections each year [1]. In addition to these morbidities and mortality, antibiotic-resistant bacteria cause significant economic losses. In the United States, the annual economic burden of *Staphylococcus aureus (S. aureus)* is as high as $13.8 billion [2]. Among them, drug-resistant *S. aureus* infection is a medical problem threatening human health and a major threat to the health of all humankind, and the formation of *S. aureus* biofilms exacerbates this threat. The infection rate and mortality rate caused by *S. aureus* biofilm infection are increasing year by year. *S. aureus* with biofilm morphology can cause various problems, including blood, respiratory infections [3], and chronic osteomyelitis [4]. One of the most dangerous infections caused by *S. aureus* is bacteremia.

The ability of biofilm formation is one of the most important virulence factors in *S. aureus,* which enables bacteria to resist or abolish the effects of different antibiotics. The genes in *S. aureus* that mainly affect the formation of biofilms are the *ica A, ica B, ica C and ica D genes,* which encode operons and surface proteins, also called biofilm-associated proteins [5]. Biofilm formation by *S. aureus* spheres greatly promotes their survival and virulence. The polysaccharide intercellular adhesin (PIA) mediates bacterial intercellular adhesion and biofilm formation [5]. PIA is produced and secreted by the proteins encoded in the intercellular adhesion (*icaABCD*) operon [6]. Among these, the *icaA* gene is thought to be responsible for biofilm production, and the *icaA*-encoded N-acetylglucosaminyltransferase

*Corresponding author. Center of Infectious Disease, West China Hospital, Sichuan University, Guoxuexiang 37, Chengdu, Sichuan, 610041, China. Tel: +86 18980601983.
E-mail: dr_liuyanbin@foxmail.com

is capable of synthesizing N-acetylglucosamine oligomers [7]. IcaB, a 259 amino acid polypeptide with a potential signal sequence, is a cell surface attachment enzyme, and IcaB is responsible for deacetylating the acetyl group of the N-acetylglucosamine molecule with PIA deacetylase activity. By deacetylation, IcaB introduces a net positive charge into PIA, which allows the polymer to attach to the bacterial surface stably. It is essential for PIA-mediated phenotypes [8]. In addition, IcaC is necessary for linking the short oligomers into longer polymer chains, and it is involved in translocation of these chains to the cell surface [9]. IcaD, together with IcaA, produces short PIA/PNAG oligomers [9].

Linezolid is a synthetic oxazolidinone antibiotic that binds to the ribosomes of bacteria and inhibits protein synthesis, thereby preventing the formation of bacterial biofilms. It has been approved as a drug for treating staphylococcal-caused skin and soft tissue infections [10]. Studies have also shown that oxazolidinone antibacterial drugs at the sub-minimum inhibitory concentration (MIC) can inhibit the formation of biofilms in drug-resistant *S. aureus*, and one of its possible mechanisms of action is that the drug may inhibit the production of exopolysaccharides by binding to IcaA and/or IcaB proteins [11].

Based on the above study, this research will focus on the molecular mechanism of linezolid against the formation of *S. aureus* biofilms and will mainly reveal the critical proteins for synthesizing the above two extracellular polysaccharides. The inhibitory mechanism of linezolid on *S. aureus* was investigated by silencing *icaA* and/or *icaB* expression in *S. aureus*. This study is expected to promote the research and development of new drugs against *S. aureus* biofilm infection and provide new ideas for the clinical treatment of *S. aureus* biofilm infection.

MATERIALS AND METHODS

Materials

Escherichia coli DH5α, *S. aureus* RN4220 and ACTT25923 and the temperature-sensitive shuttle carrier plasmid pBT2 were purchased from ATCC. Linezolid (PZ0014, SIGMA-ALDRICH), erythromycin (HY-B0220), ampicillin (HY-B0522), and chloramphenicol (HY-B0239) were purchased from MedChemExpress (New Jersey, USA). Yeast extract (lp0021) and tryptone (lp0042) were purchased from Oxoid (UK). The high-fidelity enzyme, KOD enzyme and other kits used in PCR were purchased from Vazyme (Nanjing, China). The PCR primers were synthesized by Genwiz (Suzhou, China).

Competent cell preparation

Two *S. aureus* strains, RN4220 and ATCC25923, were cultured overnight in 3–5 mL of LB, and then 1 mL of this LB solution was added to 100 mL of fresh culture medium (OD550 at 0.01). They were grown at 37 °C (shaker) to an OD550 of 0.2–0.25. It usually takes 2–2.5 h (Check OD 2 h later. The cells were checked every 15 min until the culture reached the target OD. It significantly decreased electroporation efficiency after OD550>0.3. *S. aureus* were then washed four times with 0.5 M sucrose (17% v/v) in ice, from 100 mL to 25 mL, to 10 mL, to 1 mL. A table-top centrifuge can be used, set at 9 °C and rotated at 3,000 rpm. Finally, the cells were resuspended in 500 µL 0.5 M sucrose and frozen at −80 °C.

Construction of a mutant strain of the *S. aureus ica* operon

The genomic information of *S. aureus* ATCC25923 (*S. aureus subsp. aureus* strain) was found through the NCBI website (https://www.ncbi.nlm.nih.gov/nuccore/CP009361). Primers were designed through the website https://crm.vazyme.com/cetool/multifragment.html.

Construction of the *icaA* deletion strain

Homologous recombination vectors were constructed. DNA fragments (*icaA*-up and *icaA*-down) approximately 400 bp upstream and downstream of the *icaA* gene were amplified by PCR. The erythromycin resistance gene sequence *ermB* was amplified by PCR using the engineering plasmid pMG36e as a template. Since there is a 37-bp overlapping region between the *icaA* gene CDS region and the *icaD* gene CDS region, the deletion of bases 1-1202 in the *icaA* CDS was chosen to avoid effects on *icaD* gene function.

Digestion and ligation separated these three-component amplification sequence fragments into the pBT2 vector (Table 1). This ligation product was transformed into *E. coli*

Table 1. icaA deletion primers

Primers	5′→3′
icaA-up-F-EcoRI	CGA GAA TTC CAG AAA ATT CCT CAG GCG TA
icaA-up-R-KpnI	CGG GGT ACC TTT CTT TAC CTA CCT TTC G
icaA-down-F-XbaI	TCT GTT CTA GAA TGG TCA AGC CCA GAC AGA G
icaA-down-R-HindIII	CGT AAA GCT TTC GCT TTT CTT ACA CGG TGA
ermB-F-KpnI	CGG GGT ACC ATG AAC GAG AAA AAT ATA AAA C
ermB-R-XbaI	GCG GGT CTA GAT TAC TTA TTA AAT AAT TTA TAG
Amplification 1-F	CCG GGT ACC GAG CTC GAA TTC TTC CAG AAA ATT CCT CAG GCG
Amplification 1-R	AAT TCT TTA CCT ACC TTT CGT TAG TTA GGT
Amplification 2-F	CGA AAG GTA GGT AAA GAA TTA CTT ATT AAA TAA TTT ATA GCT ATT GAA AAG AGA
Amplification 2-R	TGG GCT TGA CAT GAA CGA GAA AAA TAT AAA ACA CAG TCA
Amplification 3-F	TCT CGT TCA TGT CAA GCC CAG ACA GAG GGA A
Amplification 3-R	CAT CGC AGT GCA GCG GAA TTC GCT TTT CTT ACA CGG TGA TAA TTT AAT G

DH5α, and monoclonal strains containing the correct recombinant vector were obtained by selecting Luria-Bertani (LB) culture plates containing ampicillin. The recombinant vector was extracted and digested and verified by sequencing before use. The recombinant vector was electroporated into the *S. aureus* RN4220 strain for modification. The modified recombinant vector is not digested by the limiting enzyme system of other *S. aureus* host strains. Then, corrected recombinant mutants were screened. Monoclonal strains were selected through BHI culture plates containing erythromycin, cultured at 30 °C until the end of platform growth, and cultured overnight at 40 °C. After 100-fold dilution, they were transferred to fresh BHI culture medium overnight culture. Agar plates containing erythromycin were prepared after 100-fold dilution of overnight culture to select erythromycin-resistant and chloramphenicol-sensitive monoclonal strains. Genomic DNA from the monoclonal strains was screened and extracted, and PCR was used to verify that the correct gene deletion mutants were obtained.

Construction of the *icaB* deletion strain

Homologous recombination vectors were constructed, the primers are shown in Table 2. DNA fragments approximately 400 bp upstream and downstream of the *icaB* gene were amplified by PCR (*icaB*-up and *icaB*-down), and the erythromycin resistance gene fragment ermB was amplified by PCR using vector pMG36e as a template. (Due to the presence of a 4/14 overlap region between the *icaB* gene CDS region and the *icaD/icaC* gene CDS region, bases 5 – 859 in the *icaB CDS* were selected to avoid effects on *icaD/icaC* gene function.) The method is the same as above.

Construction of the *icaA/B* deletion strain

In the middle of the *icaA* and *icaB* genes is the *icaD* gene. Therefore, the *icaA*-up homologous fragment was first cloned into pBT2 by double digestion to obtain pBT2-*icaA*-up. Then, *icaB*-down was cloned into the vector to obtain pBT2-*icaA*-up-*icaB*-down, and then the erythromycin resistance gene fragment *ermB* and *icaD* gene fragments were cloned into pBT2-*icaA*-up-*icaB*-down to obtain pBT2-*icaA*-up-*ermB*-*icaD*-*icaB*-down. The amplification of *ermB* and *icaD* gene fragments fused the two sequences by a two-step PCR method, and the primers are shown in Table 3. Subsequent processes were as described previously. Finally, the absence of genes in the target strain was verified by PCR, and the primers are shown in Table 4.

Table 2. icaB deletion primers

Primers	5′→3′
icaB-up-F-EcoRI	CGA GAA TTC CGA GAA AAA GAA TAT GGC TGG A
icaB-up-R-KpnI	ATA GGT ACC TCA CGA TTC TCT CCC TCT CTG
icaB-down-F-XbaI	TCT GTT CTA GAA TGA AAA AGA TTA GAC TTG AAC
icaB-down-R-HindIII	CGC GAA GCT TAA AGA ATT GCA TGA TAA CAA CGA
ermB-F-KpnI	CGG GGT ACC ATG AAC GAG AAA AAT ATA AAA C
ermB-R-XbaI	GCG GGT CTA GAT TAC TTA TTA AAT AAT TTA TAG

Electrotransfer

Then, 100–160 μL of plasmid DNA was added to the competent *S. aureus*. Incubate on ice for 15 min. Add 1 μL carrier and mix well. A BIO-RAD electrotransfer instrument (Gene Pluser Xcell™, Electroporation System) was used, and electroporation conditions of 2.5 kV, 200 Ω, and 25 μF were immediately added to the test tube after electric shock, incubated at 30 °C for 2 h, placed on the appropriate antibiotic selective culture plate, and incubated in an incubator at 30 °C for 24–48 h.

Minimal inhibitory concentration

Adopt the double dilution method, and add 2 mL of liquid culture medium into 10 test tubes, in which 2 mL of linezolid (100 μg mL^{-1}) is added into the first tube. Then, successively take 2 mL from the previous gradient and add it into the next tube; discard half from the last tube, and add 0.1 mL of bacterial solution into the remaining 2 mL. The blank control without drug was used. The concentration gradients were 100, 50, 25, 12.5, 6.25, 3.125, 1.562, 0.781, 0.390, and 0.195 μg mL^{-1}, which were statically cultured in a 37 °C constant temperature incubator for 24 h. Clear sterility in the medium was used as the minimum inhibitory concentration.

Determination of the zone of inhibition

A punch printed out a circular filter paper with a diameter of 0.7 cm. After dry heat sterilization, it was added to the linezolid solution solubilized with DMSO at concentrations

Table 3. icaA and *icaB* deletion primers

Primers	5′→3′
Erm-R	GCT TGA CCA TTT ACT TAT TAA ATA ATT TAT AG
icaD-F	TAA TAA GTA AAT GGT CAA GCC CAG ACA GAG
icaD-F-xbaI	TCT GTT CTA GAT CAC GAT TCT CTC CCT CTC TG
ermB-F-KpnI	CGG GGT ACC ATG AAC GAG AAA AAT ATA AAA C
ermB-R-XbaI	GCG GGT CTA GAT TAC TTA TTA AAT AAT TTA TAG

Table 4. icaA and *icaB* deletion validation primers

Primers	5′→3′
icaA-F-104	TGA ACA AGA AGC CTG ACA T
icaA-R-404	GCA TCC AAG CAC ATT ACA TA
icaB-F-55	GTA AGC ACA CTG GAT GGT
icaB-R-791	TAA TCA TTG GAG TTC GGA GT
16S rRNA-F	GCT GCC CTT TGT ATT GTC
16S rRNA-R	AGA TGT TGG GTT AAG TCC C

of 0, 0.156, 0.3125, 1.75, 2.5, 5.0, and 10 mg mL^{-1} and pasted on an agar plate coated with ATCC 25923. The inhibition zone size was observed after 24 h of culture at 37 °C.

Biofilm formation

Add 190 µL of TSB solution to each well of a sterile 96-well plate according to reference [12] and inoculate 10 µL of a bacterial suspension with an optical density (OD595) of 0.6 in the culture medium. The blank group was treated with 10 µL DMSO, and the experimental group was treated with 10 µL linezolid solutions at concentrations of 0.4375, 0.875, 1.75, 2.5, and 5.0 mg mL^{-1}. The 96-well plates were then incubated for 16 h at 37 °C. After aspirating the bacterial solution, methanol (used as a fixative) was added to fix the biofilm. The plate was washed twice with phosphate-buffered saline and air-dried. Then, 200 µL of crystal violet solution (0.2%) was added to all wells as a dye to quantify the biofilm. After 5 min, excess crystal violet was removed, and the plate was washed twice and air-dried. Finally, the cell-bound crystal violet was solubilized using a solubilizing agent of 33% acetic acid. The absorbance at OD570 nm was measured using a microplate reader. Three wells were repeated for each concentration.

Scanning electron microscopy (SEM)

Different types of gene deletion *S. aureus* were cultured in 5 mL medium overnight (37 °C, 220 rpm), and 50 µL of 500 ng mL^{-1} linezolid solution was added to the bacterial solution the next day and cultured for another 24 h. With appropriate modifications according to the method of Boudjemaa et al. [13], the bacteria were centrifuged at 3,000 g for 10 min, and 2% glutaraldehyde solution (v/v) was added to the cell suspension at room temperature. They were then fixed for 2 h at room temperature. Afterward, glutaraldehyde was removed by rinsing three times with phosphate buffered saline for 10 min each. They were dehydrated step by step in different concentrations of ethanol (30%, 50%, 70%, 80%, 90%, and 100%), dried, and finally placed under a scanning electron microscope for observation.

Molecular docking

The 3D structure of the compound linezolid was downloaded from the PubChem database (https://pubchem.ncbi.nlm.nih.gov/). The 3D structures of IcaA and IcaB proteins were downloaded from the AlphaFold Protein Structure Database (https://alphafold.ebi.ac.uk/entry/) and PyMol was used to remove water molecules and add hydrogen atoms. AutoDock Vina 1.1.2 was used for molecular docking. Since there are no reports of relevant active sites, we used the radius of 20 units from the center of the protein as the protein active site and other parameters as the default. Finally, the conformations with the lowest docking binding energy were analysed with PyMol for docking binding mode analysis.

Statistical analysis

Statistical analysis was performed using SPSS 20.0 statistical software. The results are expressed as the mean ± standard deviation ($\overline{X} \pm$ SD). The data of two groups were compared by *t*-test, and multiple groups were compared by one-way analysis of variance (ANOVA). $P < 0.05$ was considered statistically significant.

RESULTS

Plasmid construction and gene validation

The plasmid was constructed based on *E. coli* DH5α. *icaA*-up, *icaA*-down, *icaB*-up, and *icaB*-down were amplified using the genome sequence of *S. aureus* as the template. The ermB sequence fragment was obtained by amplification using the pMG36e plasmid as a template. The PCR amplification results showed that *ermB* was obtained (Fig. 1A). The size of *ermB* was approximately 750 bp. The upstream and downstream fragments of *icaA* and *icaB* were approximately 500 bp, which was consistent with the expected results, and the band brightness was high, indicating that the product concentration could be used for subsequent experiments. The PBT2 vector was also linearized and amplified using PBT2 as a template to obtain a PBT2 linearized vector with a size of approximately 6,000 bp (Fig. 1B), which was consistent with the expected results and used in subsequent experiments. The obtained products were subjected to homologous recombination. The results are shown in Fig. 1C. The three-fragment ligation product was approximately 1,500 bp, which was consistent with the expected results, and then the bacterial solution sent for positive colonies was sequenced for further verification.

Afterward, the constructed plasmid was transferred into RN4220. Through the processing and modification of RN4220, the plasmid was more stable and not easily degraded by the host strain ATCC 25923. The three successfully constructed plasmids were transferred into ATCC 25923, and antibiotics screened the target colonies. PCR experiments were performed by designing primers and extracting bacterial DNA. The results showed that the selected strains were the same as wild-type ATCC 25923 by 16S RNA sequencing. According to the PCR results (Fig. 1D), A1 had no *icaA* fragment band, B2 had no *icaB* fragment band, and C2 had no *icaA* and *icaB* fragment position bands, indicating that these three strains had been successfully constructed.

Effect of linezolid on drug susceptibility in *ica*-silenced ATCC 25923

Through the determination of the minimum inhibitory concentration experiment, we found that turbidity still appeared in the tubes of 3.125, 1.562, 0.781, 0.390, and 0.195 µg mL^{-1}, indicating the growth of bacteria, while the culture medium was evident at a concentration of 6.25 µg mL^{-1}. Therefore, it is considered that the minimum inhibitory concentration in this experiment is 6.25 µg mL^{-1}.

Through drug testing on 96-well plates, we found that after the addition of 10 µM linezolid, the wild-type strain had no significant difference in the early inhibitory effect

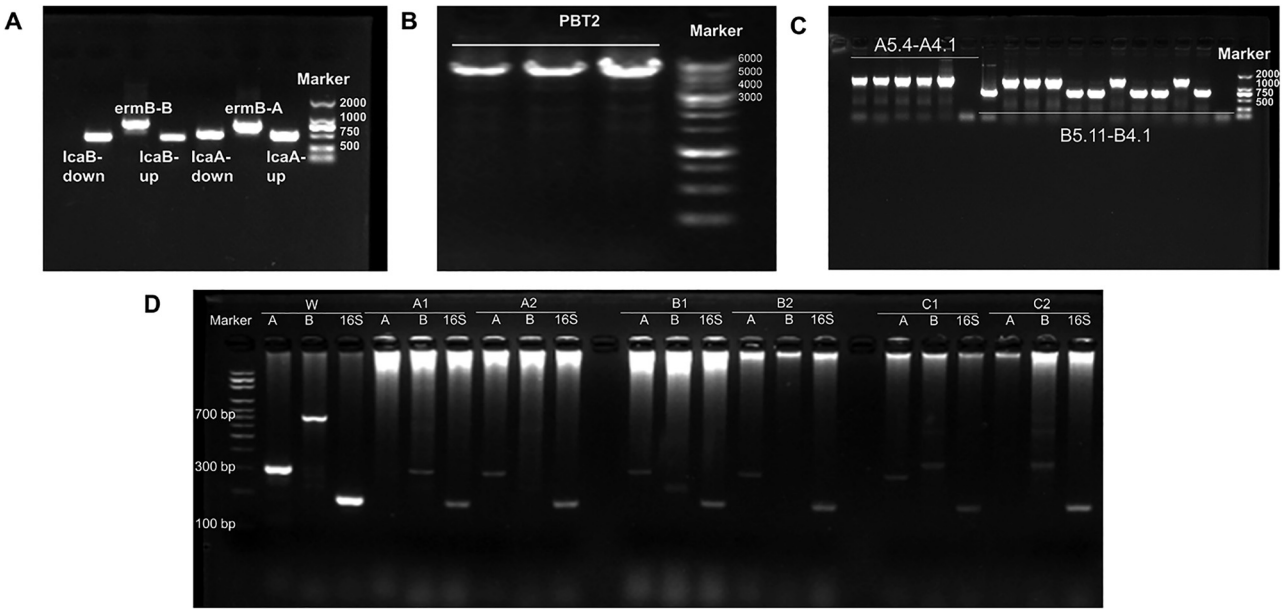

Fig. 1. PCR results. (A) PCR amplification results of *icaA*, *icaB* and *ermB*; the size of the gene fragment was expected. (B) The sequence size of the PBT2 linearized vector was approximately 6,000 bp. (C) The three-fragment ligation product size was approximately 1,500 bp, which was consistent with the expected result. (D) Homologous recombinant *S. aureus* was verified by PCR, and the results showed that A1 was missing the *icaA* fragment, B2 was missing the *icaB* sequence, and C2 was missing the *icaA* and *icaB* sequences

compared with the other three deletion strains, and after 8 h, the OD value of the deletion strain was significantly higher than that of the wild-type (Fig. 2), indicating that the inhibitory effect of the drug on deletion *S. aureus* was reduced.

As shown by the trend of inhibition zones (Fig. 3), DMSO did not affect the growth of *S. aureus*. In contrast, linezolid's inhibition of *S. aureus* increased with increasing concentration, and the inhibition zone of the deletion strain was significantly smaller than that of the wild type ($P < 0.05$). In addition, it can be found that the inhibition zone diameter of the *icaA* deletion strain is larger than that of the B deletion strain, and it is speculated that linezolid has a greater effect on *icaA* than *icaB*. There was no significant difference between the 5 mg mL^{-1} and 10 mg mL^{-1} concentrations in AB-deleted *S. aureus* ($P > 0.05$).

Effect of *ica* deficiency on biofilm formation of ATCC 25923

Through a study on the biofilm formation ability of *S. aureus*, it was found that linezolid could reduce the biofilm formation ability of *S. aureus*, and the biofilm formation ability of the deletion type was lower than that of the wild type without linezolid (0 mg mL^{-1}). In addition, strains with the *icaA* deletion had a greater decrease in biofilm competence than those with the *icaB* deletion, indicating that *icaA* had a more significant effect on biofilm formation than *icaB* (Fig. 4).

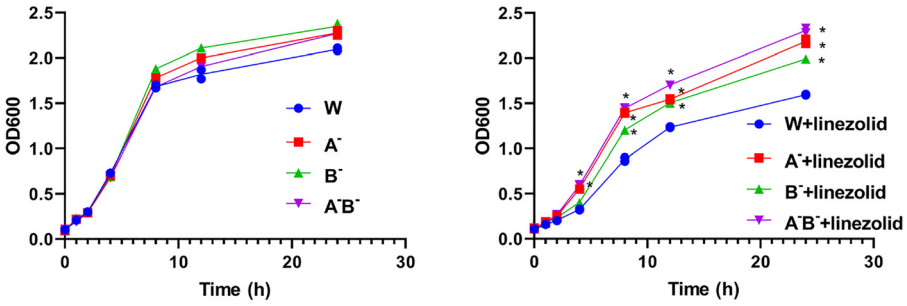

Fig. 2. Growth curves of different deletion types of *S. aureus*. No significant manufacturing differences were observed for *S. aureus* without linezolid. Growth curves differed when linezolid was added (W: wild-type strain, A^-: *icaA* deletion strain, B^-: *icaB* deletion strain, A^-B^-: *icaA and B* deletion strain). Compared with W + linezolid, * $P<0.05$

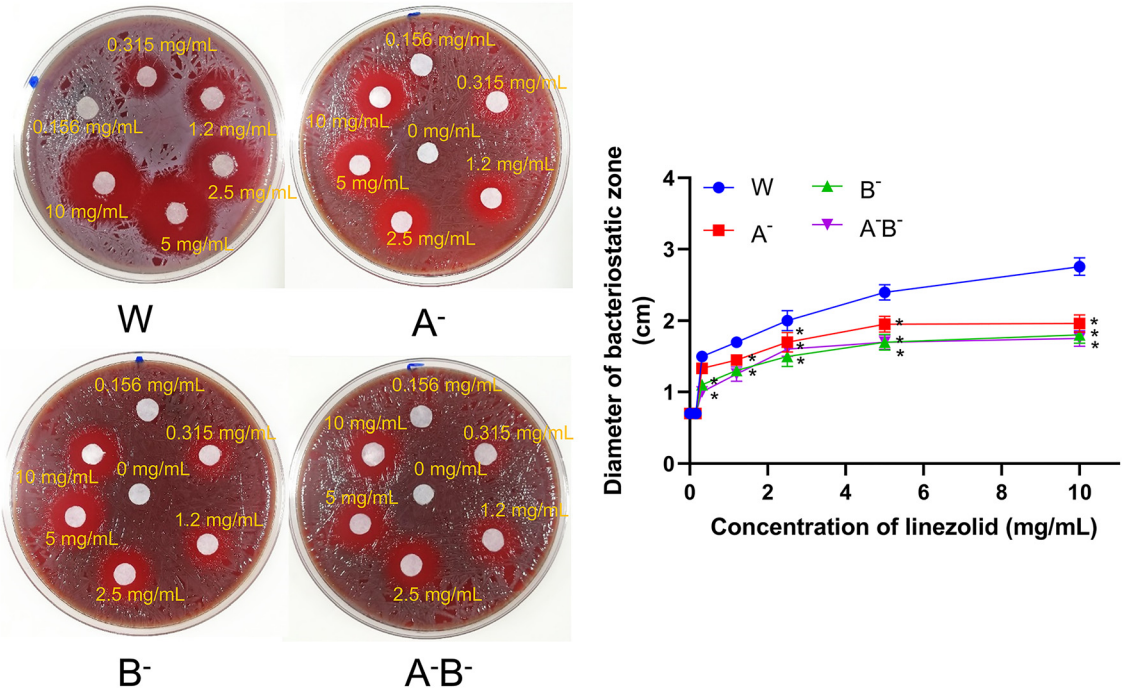

Fig. 3. Inhibition zones of linezolid against different deletion types of *S. aureus*. Wild-type *S. aureus* is most susceptible to linezolid (W: wild-type strain, A⁻: *icaA* deletion strain, B⁻: *icaB* deletion strain, A⁻B⁻: *icaA and B* deletion strain). Compared with W, * $P<0.05$

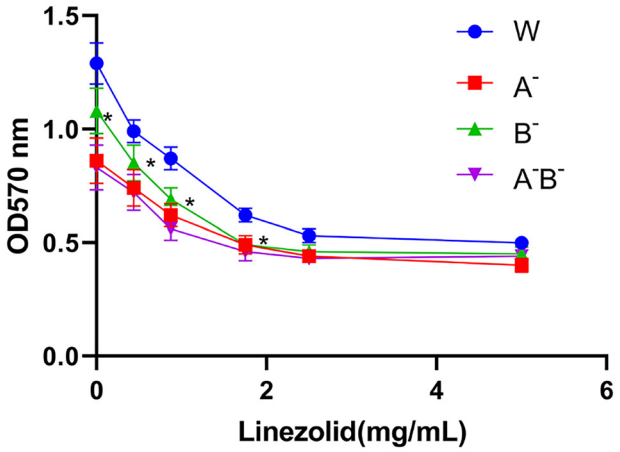

Fig. 4. Determination of the biofilm formation ability of linezolid against different deletion types of *S. aureus* (16 h). At linezolid concentrations less than 2 mg mL^{-1}, the ability of *S. aureus* biofilm formation with *ica* deletions was lower than that of the wild type. The difference was not significant at concentrations when linezolid was greater than 2 mg mL^{-1} (W: wild-type strain, A⁻: *icaA* deletion strain, B⁻: *icaB* deletion strain, A⁻B⁻: *icaA and B* deletion strain). Compared with W, * $P<0.05$

Effect of linezolid on the surface morphology of ATCC 25923

As shown in Fig. 5, a dense biofilm is formed in wild-type *S. aureus*, and the addition of linezolid damages the bacterial surface. This showed that linezolid was indeed able to affect the surface morphology of *S. aureus*, leading to the rupture of some bacterial individuals and thereby inhibiting bacterial growth. It was found that the adhesion between bacteria decreased to some extent after drug addition, with no significant bonding between bacterial individuals.

Molecular docking results

According to the molecular docking results, linezolid can bind the IcaA and IcaB proteins with binding energies of −7.9 kcal mol^{-1} and −5.0 kcal mol^{-1}, respectively, and linezolid presents better binding ability to IcaA. In addition, as seen from the 2D interaction plot, linezolid forms hydrogen bonds with the amino acid residue Asp227 of IcaA (Fig. 6A), forming a hydrophobic interaction with Trp267. There are van der Waals forces with amino acid residues Val383, Asn380, Val384, Ala268, Thr200, Ile228, Gly203, Val204, Tyr181, Ser202, Ile185, Pro164, Arg264, and Asn199. It forms hydrogen bonds with amino acid residues Leu252 of IcaB and van der Waals forces with Met233, Leu232, Gly231, Tyr230, Tyr75, Glu253, Ser251, Asn74, Leu270, and Glu254 (Fig. 6B).

DISCUSSION

S. aureus can cause various infections, such as skin and soft tissue injuries to fatal conditions, osteomyelitis, endocarditis, pneumonia, and sepsis [14]. In recent years, the morbidity and mortality of diseases caused by *S. aureus* have increased significantly, seriously endangering human life and health, mainly due to bacterial resistance. While biofilm formation is a significant cause of increased bacterial resistance,

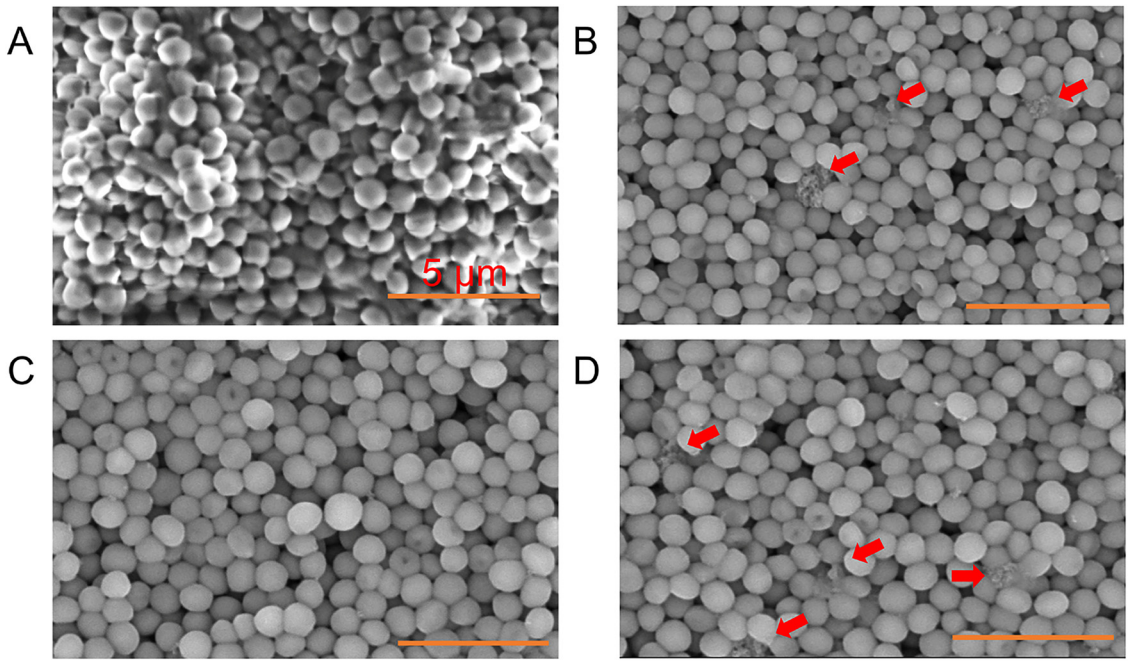

Fig. 5. SEM was performed to observe the effect of linezolid on the proliferation of *S. aureus*. (A) Wild type. (B) Wild type + linezolid. (C) *icaA* deletion + linezolid. (D) *icaB* deletion + linezolid

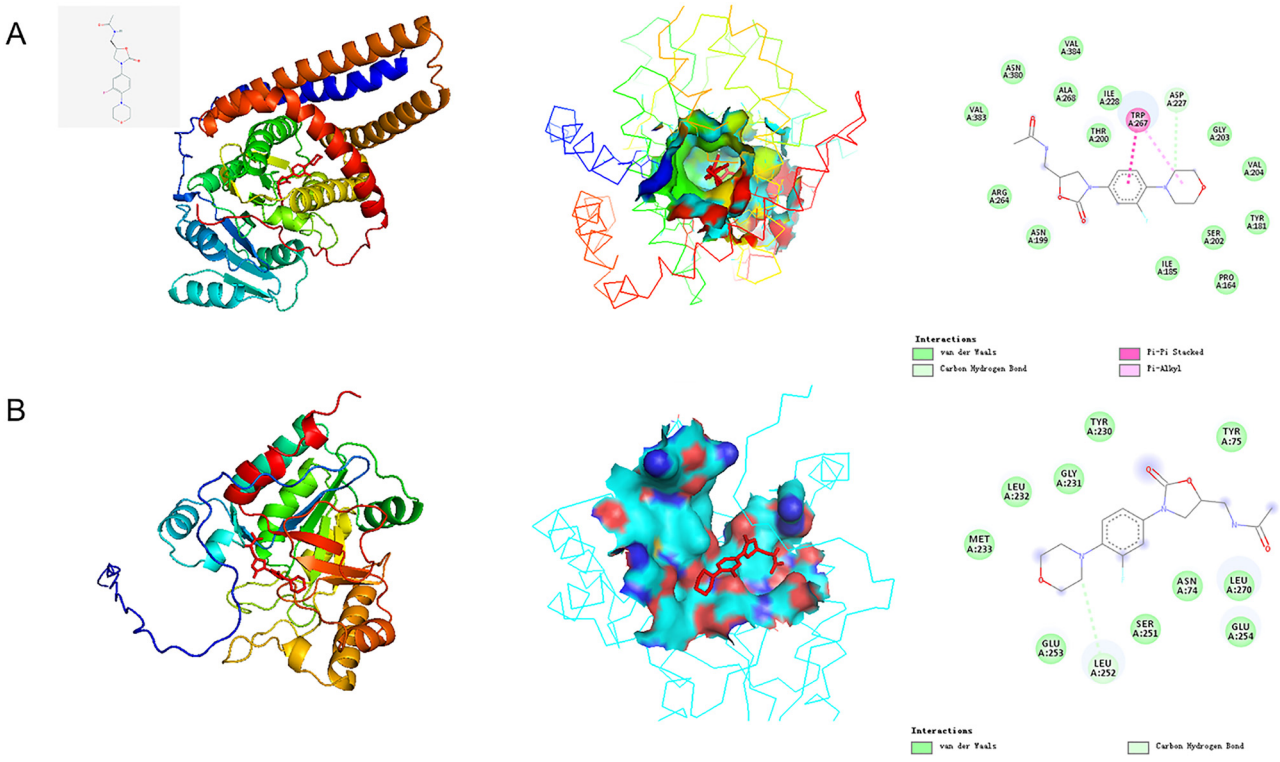

Fig. 6. Molecular docking results. (A) Linezolid forms hydrogen bonds with amino acid residue Asp227 of IcaA, forming a hydrophobic interaction with Trp267. (B) Linezolid forms hydrogen bonds with amino acid residue Leu252 of IcaB

S. aureus biofilm formation can act as a natural barrier against bacteriostatic agents [15, 16]. The mechanism of biofilm production in staphylococci is related to the synthesis of the polysaccharide intercellular adhesin PIA by the intercellular adhesion gene cluster (*icaADBC*) [17, 18]. *IcaA* is a transmembrane glucosyltransferase, which together with *icaD* produces short PIA/poly-N-acetyl-β-(1-6)-glucosamine (PNAG) oligomers [19]. IcaB is responsible for the partial

deacetylation of PIA/PNAG molecules, which are necessary for retention on the cell surface [20]. The *icaA* gene is found in many environments in *S. aureus*, and in animals, *icaA* is detected in greater than 40% of *S. aureus* [21]. Some studies have even found that *icaA* accounted for the highest detection rate of *S. aureus* detected in milk, up to 63.3%, and developed drug resistance [22]. In methicillin-resistant *S. aureus*, increased expression of *ica* is a major cause of biofilm formation capacity [23]. Therefore, this study will focus on IcaA and IcaB, two critical proteins in synthesizing extracellular polysaccharides. To survey the molecular mechanism of linezolid against the formation of *S. aureus* biofilms. At the same time, a new target for IcaA and Ica B by linezolid was sought to provide a research basis for the preclinical evaluation of antimicrobial biofilm drugs. Ultimately, it provides a new strategy for the treatment of infections against drug-resistant *S. aureus*.

In this study, we first constructed defective plasmids and detected the essential biological functions of these three strains after silencing the *icaA, icaB*, and *icaA/B* genes of *S. aureus* and found that the growth rate of *S. aureus* was inhibited under the action of the drug line zolid. However, the growth rate of defective *S. aureus* was significantly increased compared with that of the wild type. These results suggest that IcaA and IcaB may be drug targets of linezolid. The drug's inhibition rate of *S. aureus* growth decreased after deleting these two essential target proteins. This result suggests that linezolid can inhibit the growth of *S. aureus* to some extent by targeting IcaA/B. From the biofilm formation assay, the biofilm formation ability of the defective strain was significantly decreased compared with that of the wild type. It is concluded that linezolid can reduce the ability of *S. aureus* biofilm formation to some extent, thereby indirectly inhibiting biofilm formation. Previous studies have found that the *ica* locus is conserved between *Staphylococcus epidermidis* and *S. aureus*. In contrast to *S. epidermidis*, in vitro, PIA production and biofilm formation are evident in most *S. aureus* strains. They are often observed only under stringent in vitro conditions, such as low oxygen [24]. This also contributes to the low biofilm formation capacity we observed for *S. aureus*.

Our experiments also found that linezolid significantly differed in inhibitory ability on broth medium and agar plates. Since bacteria grown in flat biofilms are very different from the same bacteria grown in suspension culture, they have different growth environments and growth characteristics and absorb nutrients and drugs in different ways [25]. This leads to some differences in the inhibitory ability of the drug against bacteria. In addition, antimicrobials can prevent bacterial adhesion when exposed to bacteria before biofilm formation [26]. This also resulted in a higher colony-forming ability on the plates than on the colonies in the broth. In addition, in this study, we observed control and *icaA*- and *icaB*-silenced *S. aureus* by scanning electron microscopy and found that control bacteria presented normal cell morphology and showed biofilm appearance. In contrast, silenced bacteria showed biofilm reduction and bacterial rupture after linezolid treatment. Some bacterial cells exhibit deep pits on their cell walls, which is similar to the study by El-Nagdy et al. [7].

Drug-resistant *S. aureus* biofilm infection is a medical problem threatening human health. Due to the lack of an anti-biofilm drug evaluation system and the study of the molecular mechanism of *S. aureus* biofilm formation, resulting in the absence of therapeutic means, there is blindness and uncertainty in the search for drugs. The above studies preliminarily concluded that linezolid could inhibit IcaA and IcaB, critical proteins of *S. aureus* biofilm formation. Nevertheless, the specific active sites of IcaA and IcaB could not be determined in the current study. We predicted the potential binding effect of linezolid by molecular simulation and found that linezolid has a higher critical ability for IcaA than IcaB, but this also needs to be verified in the future. Moreover, the emergence of strains carrying linezolid resistance genes has recently been reported, drawing more attention to combating *S. aureus* [27]. Therefore, we need to elucidate the mechanism of action of linezolid to provide a reference for the development of drugs in the future.

CONCLUSION

In this study, we investigated the effect of linezolid on the above two biofilm formation-related target proteins by silencing *icaA* and *icaB* and found that linezolid could inhibit the growth of *S. aureus* and biofilm formation to some extent, which may be related to targeting IcaA and IcaB proteins. This study provides a research basis for linezolid inhibition of *S. aureus* biofilm formation and provides a new strategy for infection treatment against drug-resistant *S. aureus*.

DECLARATIONS

Availability of data and material: The datasets used and/or analysed during the current study are available from the corresponding author on reasonable request.

Competing interests: All the authors declare that they have no conflicts of interest.

Funding: This work was supported by grants obtained from Sichuan Science and Technology Department Support Plan (2018SZ0017).

Author contributions: HX B and YB L contributed to the study conception and design. All authors collected the data and performed the data analysis. All authors contributed to the interpretation of the data and the completion of figures and tables. All authors contributed to the drafting of the article and final approval of the submitted version.

Ethics statement: Not applicable.

ACKNOWLEDGMENTS

None.

REFERENCES

1. Cassini A, Högberg LD, Plachouras D, Quattrocchi A, Hoxha A, Simonsen GS, et al. Attributable deaths and disability-adjusted life-years caused by infections with antibiotic-resistant bacteria in the EU and the European Economic Area in 2015: a population-level modelling analysis. Lancet Infect Dis 2019; 19(1): 56–66.
2. Lee BY, Singh A, David MZ, Bartsch SM, Slayton RB, Huang SS, et al. The economic burden of community-associated methicillin-resistant Staphylococcus aureus (CA-MRSA). Clin Microbiol Infect 2013; 19(6): 528–36.
3. David MZ, Daum RS. Treatment of Staphylococcus aureus infections. Curr Top Microbiol Immunol 2017; 409: 325–83.
4. Hamahashi K, Uchiyama Y, Kobayashi Y, Watanabe M. Delayed methicillin-resistant Staphylococcus aureus-induced osteomyelitis of the tibia after pin tract infection: two case reports. J Med Case Rep 2017; 11(1): 23.
5. Kadkhoda H, Ghalavand Z, Nikmanesh B, Kodori M, Houri H, Taghizadeh Maleki D, et al. Characterization of biofilm formation and virulence factors of Staphylococcus aureus isolates from paediatric patients in Tehran, Iran. Iran J Basic Med Sci 2020; 23(5): 691–8.
6. Hait JM, Cao G, Kastanis G, Yin L, Pettengill JB, Tallent SM. Evaluation of virulence determinants using whole-genome sequencing and phenotypic biofilm analysis of outbreak-linked Staphylococcus aureus isolates. Front Microbiol 2021; 12: 687625.
7. El-Nagdy AH, Abdel-Fattah GM, Emarah Z. Detection and control of biofilm formation by Staphylococcus aureus from febrile neutropenic patient. Infect Drug Resist 2020; 13: 3091–101.
8. Nguyen HTT, Nguyen TH, Otto M. The staphylococcal exopolysaccharide PIA - biosynthesis and role in biofilm formation, colonization, and infection. Comput Struct Biotechnol J 2020; 18: 3324–34.
9. Brooks JL, Jefferson KK. Phase variation of poly-N-acetylglucosamine expression in Staphylococcus aureus. Plos Pathog 2014; 10(7): e1004292.
10. Herrmann DJ, Peppard WJ, Ledeboer NA, Theesfeld ML, Weigelt JA, Buechel BJ. Linezolid for the treatment of drug-resistant infections. Expert Rev Anti Infect Ther 2008; 6(6): 825–48.
11. Edwards GA, Shymanska NV, Pierce JG. 5-Benzylidene-4-oxazolidinones potently inhibit biofilm formation in Methicillin-resistant Staphylococcus aureus. Chem Commun (Camb) 2017; 53(53): 7353–6.
12. Leoney A, Karthigeyan S, Asharaf AS, Felix AJW. Detection and categorization of biofilm-forming Staphylococcus aureus, Viridans streptococcus, Klebsiella pneumoniae, and Escherichia coli isolated from complete denture patients and visualization using scanning electron microscopy. J Int Soc Prev Community Dent 2020; 10(5): 627–33.
13. Boudjemaa R, Steenkeste K, Canette A, Briandet R, Fontaine-Aupart MP, Marlière C. Direct observation of the cell-wall remodeling in adhering Staphylococcus aureus 27217: an AFM study supported by SEM and TEM. Cell Surf 2019; 5: 100018.
14. Gowrishankar S, Kamaladevi A, Balamurugan K, Pandian SK. In vitro and in vivo biofilm characterization of methicillin-resistant Staphylococcus aureus from patients associated with pharyngitis infection. Biomed Res Int 2016; 2016: 1289157.
15. Qu D, Hou Z, Li J, Luo L, Su S, Ye Z, et al. A new coumarin compound DCH combats methicillin-resistant Staphylococcus aureus biofilm by targeting arginine repressor. Sci Adv 2020; 6(30): eaay9597.
16. Sharma D, Misba L, Khan AU. Antibiotics versus biofilm: an emerging battleground in microbial communities. Antimicrob Resist Infect Control 2019; 8: 76.
17. McCarthy H, Rudkin JK, Black NS, Gallagher L, O'Neill E, O'Gara JP. Methicillin resistance and the biofilm phenotype in Staphylococcus aureus. Front Cell Infect Microbiol 2015; 5: 1.
18. Zapotoczna M, O'Neill E, O'Gara JP. Untangling the diverse and redundant mechanisms of Staphylococcus aureus biofilm formation. Plos Pathog 2016; 12(7): e1005671.
19. Gerke C, Kraft A, Süssmuth R, Schweitzer O, Götz F. Characterization of the N-acetylglucosaminyltransferase activity involved in the biosynthesis of the Staphylococcus epidermidis polysaccharide intercellular adhesin. J Biol Chem 1998; 273(29): 18586–93.
20. Vuong C, Kocianova S, Voyich JM, Yao Y, Fischer ER, DeLeo FR, et al. A crucial role for exopolysaccharide modification in bacterial biofilm formation, immune evasion, and virulence. J Biol Chem 2004; 279(52): 54881–6.
21. Mello PL, Riboli DFM, Martins LA, Brito M, Victória C, Calixto Romero L, et al. Staphylococcus spp. isolated from bovine subclinical mastitis in different regions of Brazil: molecular typing and biofilm gene expression analysis by RT-qPCR. Antibiotics (Basel) 2020; 9(12).
22. Bissong MEA, Ateba CN. Genotypic and phenotypic evaluation of biofilm production and antimicrobial resistance in Staphylococcus aureus isolated from milk, north west province, South Africa. Antibiotics (Basel) 2020; 9(4).
23. Tahmasebi H, Dehbashi S, Jahantigh M, Arabestani MR. Relationship between biofilm gene expression with antimicrobial resistance pattern and clinical specimen type based on sequence types (STs) of methicillin-resistant S. aureus. Mol Biol Rep 2020; 47(2): 1309–20.
24. Fluckiger U, Ulrich M, Steinhuber A, Döring G, Mack D, Landmann R, et al. Biofilm formation, icaADBC transcription, and polysaccharide intercellular adhesin synthesis by staphylococci in a device-related infection model. Infect Immun 2005; 73(3): 1811–9.
25. El-Azizi M, Rao S, Kanchanapoom T, Khardori N. In vitro activity of vancomycin, quinupristin/dalfopristin, and linezolid against intact and disrupted biofilms of staphylococci. Ann Clin Microbiol Antimicrob 2005; 4: 2.
26. Yassien M, Khardori N. Interaction between biofilms formed by Staphylococcus epidermidis and quinolones. Diagn Microbiol Infect Dis 2001; 40(3): 79–89.
27. Michalik M, Kosecka-Strojek M, Wolska M, Samet A, Podbielska-Kubera A, Międzobrodzki J. First case of staphylococci carrying linezolid resistance genes from laryngological infections in Poland. Pathogens 2021; 10(3).